

The inhibition of photosynthesis under water deficit conditions is more severe in flecked than uniform irradiance in rice (*Oryza sativa*) plants

Jiali Sun^A, Qiangqiang Zhang^A, Muhammad Adnan Tabassum^A, Miao Ye^A, Shaobing Peng^A and Yong Li^{A,B}

^AMinistry of Agriculture Key Laboratory of Crop Ecophysiology and Farming System in the Middle Reaches of the Yangtze River, College of Plant Science and Technology, Huazhong Agricultural University, No.1, Shizishan Street, Wuhan, Hubei 430 070, China.

^BCorresponding author. Email: liyong@mail.hzau.edu.cn

Abstract. Water deficit is considered the major environmental factor limiting leaf photosynthesis, and the physiological basis for decreased photosynthesis under water deficit has been intensively studied with steady irradiance. Leaves within a canopy experience a highly variable light environment in magnitude and time, but the effect of water deficit on photosynthesis in fluctuating irradiance is not well understood. Two rice cultivars with different drought tolerance, Champa and Yangliangyou 6 (YLY6), were hydroponically grown under well-watered, 15% (m/v) and 20% PEG (polyethylene glycol, 6000 Da) induced water deficit conditions. The inhibition of steady-state photosynthesis in Champa is more severe than YLY6. The maximum Rubisco carboxylation capacity (V_{cmax}) and maximum electron transport capacity (J_{max}) were decreased under 20% PEG treatment in Champa, whereas less or no effect was observed in YLY6. The induction state ($IS\%$, which indicates photosynthesis capacity after exposure of low-light period) of both leaf photosynthetic rate (A) and stomatal conductance (g_s) was highly correlated, and was significantly decreased under water deficit conditions in both cultivars. Water deficit had no significant effect on the time required to reach 50 or 90% of the maximum photosynthetic rate ($T_{50\%,A}$ and $T_{90\%,A}$) after exposure to high-light level, but significantly led to a greater decrease in photosynthetic rate in the low-light period under flecked irradiance ($A_{\text{min-fleck}}$) relative to photosynthetic rate in the same light intensity of continuously low-light period (A_{initial}). The lower $IS\%$ of A and more severe decrease in $A_{\text{min-fleck}}$ relative to A_{initial} will lead to a more severe decrease in integrated CO_2 fixation under water deficit in flecked compared with uniform irradiance.

Additional keywords: dynamic photosynthesis, induction state, simulated sunflecks, steady-state photosynthesis, stomatal conductance, water deficit.

Received 16 April 2016, accepted 22 December 2016, published online 3 February 2017

Introduction

Studies of photosynthesis are mostly conducted under steady-state conditions. However, steady-state conditions are rare in nature, and growth environments, especially irradiance, are inherently heterogeneous in time and space within canopies (Percy *et al.* 1990; Lawson *et al.* 2012). At any given level in the canopy, gaps between the leaves in the layer above produce sunflecks that may change rapidly in size and photosynthetic photon flux density (PPFD) because of the wind (Percy *et al.* 1990; Timm *et al.* 2002; Lawson *et al.* 2012). Involving many subprocesses, photosynthesis cannot respond linearly to changing irradiance. Therefore, in order to understand photosynthesis in natural conditions, it is important to investigate in conditions of fluctuating irradiance, namely, dynamic photosynthesis.

Previous studies on dynamic photosynthesis have focussed on the influences of changing irradiance on photosynthetic subprocesses, including electron and proton transport, non-photochemical quenching, RuBP regeneration, activation of Calvin cycle enzymes, and stomatal opening (Lawson *et al.* 2012; Kaiser *et al.* 2015). The effect of environmental factors on dynamic photosynthesis is less well known; only a handful of studies have focussed on the influence of elevated CO_2 concentration, leaf temperature, and air humidity on dynamic photosynthesis (Leakey *et al.* 2002, 2003; Cui *et al.* 2009). The lack of knowledge in this area will restrict the understanding of photosynthesis in natural conditions, because plants are usually grown under suboptimal conditions.

Water deficit is considered the major environmental factor limiting plant growth and productivity, because it decreases leaf

photosynthetic rate (A). The physiological basis for decreased photosynthesis under drought has been well documented. Stomatal closure in response to drought restricts CO_2 entry, and thereby limits photosynthesis as well as decreasing water loss. It is suggested that stomatal closure is the earliest and the dominant response to drought during mild and moderate water deficit (Flexas and Medrano 2002; Flexas *et al.* 2002), whereas limitations from mesophyll conductance and biochemical capacities (e.g. RuBP regeneration rate, ATP synthesis, Rubisco activity) are progressively improved during severe and long-term water deficit (Parry *et al.* 2002; Cano *et al.* 2014; Perez-Martin *et al.* 2014). But the influence of water deficit on dynamic photosynthesis has not been studied.

To efficiently use energy, the leaves need to maintain a relatively high photosynthesis induction state ($IS\%$) and stomatal conductance (g_s) under shade or low-light periods of flecked irradiance. With regard to stomatal movement during sunflecks, water deficit might be expected to reduce the rate of stomatal opening in response to increasing irradiance, and to increase the rate of stomatal closure with decreasing irradiance (Way and Pearcy 2012). Moreover, many studies show that stomatal conductance under uniform irradiance ($g_{s,\text{steady}}$) is strongly and negatively related to the time required to reach 50 or 90% of the maximum photosynthetic rate ($T_{50\%,A}$ and $T_{90\%,A}$), when shifting from low- to high-light levels (Valladares *et al.* 1997; Allen and Pearcy 2000; Wong *et al.* 2012). This suggests that the plant with a low g_s under water deficit conditions may require more time for photosynthesis to recover when shifting from low to high irradiance, which will inevitably aggravate the negative effect of water deficit on photosynthesis.

However, the negative correlation between $g_{s,\text{steady}}$ and $T_{50\%,A}$ (or $T_{90\%,A}$) is mostly found when the $g_{s,\text{steady}}$ is lower than a threshold value, which is usually lower than $0.1 \text{ mol m}^{-2} \text{ s}^{-1}$ (Valladares *et al.* 1997; Allen and Pearcy 2000), although Wong *et al.* (2012) found the negative correlation also exists when $g_{s,\text{steady}}$ reaches $\sim 0.4 \text{ mol m}^{-2} \text{ s}^{-1}$. Growing in paddy fields, g_s of rice plants is usually higher than $0.4 \text{ mol m}^{-2} \text{ s}^{-1}$ (Hubbart *et al.* 2007). Whether the decrease in g_s of rice plants under water deficit can lead to a longer $T_{50\%,A}$ or $T_{90\%,A}$, and subsequently lead to a more severe decrease in photosynthesis is not known.

In the present study, rice seedlings were hydroponically grown under three water statuses: well-watered conditions, 15% (m/v) and 20% PEG (polyethylene glycol, 6000 Da) induced water deficit conditions. Both steady-state and dynamic photosynthesis were measured to (1) study the effects of water deficit on photosynthesis under both steady-state and flecked irradiance; and (2) investigate whether flecked irradiance treatments can aggravate the negative effect of water deficit on photosynthesis. This was done by studying the effects of water deficit on the response of $IS\%$ to low-light duration and on the time required for photosynthesis induction after shifting from low- to high-light level.

Materials and methods

Plant materials and water treatments

After germination on moist filters on 21 August 2015, seeds of two rice cultivars with different drought tolerance, Champa and

Yangliangyou 6 (YLY6), were transferred to nursery plates. Thirteen days after germination, when the seedlings had developed an average of 2.5 leaves, they were transplanted to 11.0 L pots with a density of eight hills per pot and two seedlings per hill. The seedlings were supplied with full-strength Hoagland solution. Ten days later, water stress was simulated on the partial seedlings by adding PEG to a final concentration of 10% in the nutrient solutions. Eight days later, PEG concentrations were increased to 15% or 20%. Twelve days later, gas-exchange measurements were started. In total there were three treatments (well-watered condition, 15 and 20% PEG induced water deficit conditions), and three pots per treatment. The pots were placed randomly to avoid edge effects.

The composition of the nutrients in solutions was as follows: macronutrients (mg L^{-1}): 40 N as equal moles of $(\text{NH}_4)_2\text{SO}_4$ and $\text{Ca}(\text{NO}_3)_2$, 10 P as KH_2PO_4 , 40 K as K_2SO_4 and KH_2PO_4 , 40 Mg as MgSO_4 ; micronutrients (mg L^{-1}): 2.0 Fe as Fe-EDTA, 0.5 Mn as $\text{MnCl}_2 \cdot 4\text{H}_2\text{O}$, 0.05 Mo as $(\text{NH}_4)_6\text{Mo}_7\text{O}_{24} \cdot 4\text{H}_2\text{O}$, 0.2 B as H_3BO_3 , 0.01 Zn as $\text{ZnSO}_4 \cdot 7\text{H}_2\text{O}$, 0.01 Cu as $\text{CuSO}_4 \cdot 5\text{H}_2\text{O}$, 2.8 Si as $\text{Na}_2\text{SiO}_3 \cdot 9\text{H}_2\text{O}$. Nutrient solutions were changed every 3 days, and pH was adjusted to 5.50 ± 0.05 every day with 0.1 mol L^{-1} HCl or 0.1 mol L^{-1} NaOH.

Gas-exchange measurements

CO_2 response curve measurement

All gas exchange measurements were conducted on the newest fully expanded leaves using a portable photosynthesis system (LI-6400XT; Li-Cor Inc.) between 0900 and 1600 hours. Prior to the measurements for CO_2 response curves, leaves were placed in the leaf chamber for at least 15 min at a PPFD of $1500 \mu\text{mol m}^{-2} \text{ s}^{-1}$, a CO_2 concentration in the reference chamber of $400 \mu\text{mol mol}^{-1}$ with a CO_2 mixture, a leaf temperature of 28°C , and a leaf-to-air vapour pressure deficit (VPD) of 1 kPa. After equilibration to a steady-state, data were recorded and the leaf photosynthesis and stomatal conductance measured were defined as the steady-state photosynthesis (A_{steady}) and $g_{s,\text{steady}}$. Thereafter, CO_2 concentration in the reference chamber was controlled across a series of 400, 200, 150, 100, 50, 25, 400, 600, 800, 1000 and $1500 \mu\text{mol mol}^{-1}$ with a CO_2 mixture to measure the CO_2 response curves. Carboxylation efficiency (CE) was calculated by linear regression of the data points when the CO_2 concentration in the reference chamber was $\leq 200 \mu\text{mol mol}^{-1}$.

Measurement of mesophyll conductance

Gas exchange and chlorophyll fluorescence were simultaneously measured using LI-6400XT equipped with a 6400-40 leaf chamber. CO_2 in the reference chamber was controlled to $400 \mu\text{mol mol}^{-1}$ with a CO_2 mixture, leaf temperature, VPD and PPFD were controlled to the same as mentioned above. After equilibration to a steady-state, the steady-state fluorescence (F_s) was measured and a 0.8 s saturating pulse of light ($\sim 8000 \mu\text{mol m}^{-2} \text{ s}^{-1}$) was applied to measure the maximum fluorescence (F_m'). Gas-exchange data were also recorded simultaneously. The photosynthetic efficiency of photosystem (Φ_{PSII}) was calculated as:

$$\Phi_{\text{PSII}} = 1 - \frac{F_s}{F_m}. \quad (1)$$

The electron transport rate of PSII (J) was calculated as:

$$J = \text{PPFD} \times \Phi_{\text{PSII}} \times \alpha \times \beta, \quad (2)$$

where α and β are leaf absorption and the proportion of quanta absorbed by PSII, respectively. The product $\alpha \times \beta$ was determined from the slope of relationship between Φ_{PSII} and the quantum efficiency of CO_2 uptake (Φ_{CO_2}), obtained by varying light intensity under non-photorespiratory conditions at less than 2% O_2 (Valentini *et al.* 1995).

The variable J method was used to calculate g_m using the equation:

$$g_m = \frac{A}{C_i - \frac{\Gamma^* \times (J + 8(A + R_d))}{J - 4(A + R_d)}}, \quad (3)$$

where Γ^* and R_d are the CO_2 compensation point in the absence of respiration and mitochondrial respiration rate in the light respectively. Γ^* and R_d were measured following Laisk's method, as described Li *et al.* (2012).

The chloroplastic CO_2 concentration (C_c) was calculated as:

$$C_c = C_i - \frac{A}{g_m}. \quad (4)$$

Calculations of V_{cmax} and J_{max}

A/C_c curves were estimated from A/C_i curves with the corresponding g_m , the maximum Rubisco carboxylation capacity (V_{cmax}) and maximum electron transport capacity (J_{max}) were calculated according to the models described by the Farquhar *et al.* (1980) and Sharkey (2016). Generally, V_{cmax} was calculated under the assumption that photosynthesis was limited by Rubisco carboxylation at C_i values below $200 \mu\text{mol mol}^{-1}$ (Sharkey *et al.* 2007). At these low CO_2 values, A was fitted to the Rubisco-limited process:

$$A = V_{\text{cmax}} \times \frac{C_c - \Gamma^*}{C_c - K_c(1 + O/K_o)} - R_d, \quad (5)$$

where K_c and K_o are the Michaelis-Menten constants for CO_2 and O_2 , O is the partial pressure of O_2 ($0.21 \text{ mol mol}^{-1}$). The K_c and K_o measured by Bernacchi *et al.* (2002) were used in the calculation of V_{cmax} and J_{max} . The temperature response of K_c and K_o were calculated as:

$$\text{Parameter} = \exp\left(c - \frac{\Delta H_a}{RT_k}\right), \quad (6)$$

where c is a scaling constant, ΔH_a is the energy of activation, R is the molar gas constant ($8.314 \text{ JK}^{-1} \text{ mol}^{-1}$) and T_k is the leaf temperature in Kelvin. The scaling constant and the energy of activation were also taken from Bernacchi *et al.* (2002). This allows the calculation of K_c and K_o at 28°C , where leaf photosynthesis was measured in the present study. J_{max} was calculated under the assumption that photosynthesis was limited by RuBP regeneration at C_i values above $300 \mu\text{mol mol}^{-1}$ (Sharkey *et al.* 2007). At these high CO_2 values, A was fitted to the RuBP regeneration process:

$$A = J_{\text{max}} \times \frac{C_c - \Gamma^*}{4C_c + 8\Gamma^*} - R_d. \quad (7)$$

Measurement of induction state

The response time of the gas-exchange apparatus was checked before the measurement of the dynamic gas exchange, and a quick response time of 5 s at the flow rate of 500 mL min^{-1} was observed, which was similar to that in other studies (Leakey *et al.* 2002, 2003). Estimations of the $IS\%$, the time required for photosynthesis induction (T_{50} and T_{90}), the post-irradiance CO_2 fixation (PIF) and CO_2 burst (PIB) were calculated after raw output was corrected for the system lag time.

The response of $IS\%$ to various duration of the low-light exposures was measured according to the procedure described in Fig. S1a (available as Supplementary Material to this paper) and also by Sun *et al.* (2016). Briefly, photosynthesis of the newly expanded leaves was first induced under light-saturated conditions ($\text{PPFD} = 1500 \mu\text{mol m}^{-2} \text{ s}^{-1}$) for at least 15 min, which is long enough for photosynthesis to be fully induced, then the data were automatically recorded every 2 s. The A and g_s here were similar to A_{steady} and $g_{s,\text{steady}}$ calculated from CO_2 response curves, because they were both fully induced at $1500 \mu\text{mol m}^{-2} \text{ s}^{-1}$ for at least 15 min. Three minutes after recording, the light was decreased immediately to $100 \mu\text{mol m}^{-2} \text{ s}^{-1}$. One minute later, the light was increased immediately to $1500 \mu\text{mol m}^{-2} \text{ s}^{-1}$ for the leaves to be fully induced again, which needed 5 min. Thereafter, the light was decreased immediately to $100 \mu\text{mol m}^{-2} \text{ s}^{-1}$. Five minutes later, the light was again increased to $1500 \mu\text{mol m}^{-2} \text{ s}^{-1}$. Ten minutes later, the light was again decreased to $100 \mu\text{mol m}^{-2} \text{ s}^{-1}$. Another 10 minutes later, the light was increased to $1500 \mu\text{mol m}^{-2} \text{ s}^{-1}$. Fifteen minutes later, the procedure of measurement was stopped. Therefore, there were three low-light periods, the durations of which were 1, 5 and 10 min respectively. After each low-light period, 5, 10 and 15 min of high-light were long enough for leaves to be fully induced. The $IS\%$ value of A was calculated as:

$$IS\% \text{ of } A = \frac{A_{30} + R_d}{A_{\text{steady}} + R_d}, \quad (8)$$

where A_{30} is the instantaneous photosynthetic rate 30 s after switching from low- to high-light levels. The instantaneous g_s 30 s after switching from low- to high-light levels was referred to as $g_{s,30}$, and the $IS\%$ value of g_s can be calculated as:

$$IS\% \text{ of } g_s = \frac{g_{s,30}}{g_{s,\text{steady}}}. \quad (9)$$

Measurement of dynamic photosynthesis in flecked irradiance

The photosynthetic induction process was measured according to the procedure described in Fig. S1b and by Sun *et al.* (2016). Briefly, seedlings were kept in darkness by placing them in a controlled growth chamber ($\text{PPFD} 0 \mu\text{mol m}^{-2} \text{ s}^{-1}$; temperature 28°C ; RH 60%; CO_2 concentration $400 \mu\text{mol mol}^{-1}$) from 2000 hours on the previous day until the measurement was started at 0900 hours. After a prolonged low-light of $100 \mu\text{mol m}^{-2} \text{ s}^{-1}$ (>15 min), the data were automatically

recorded for 3 min. The A and g_s here were referred as A_{initial} and $g_{s,\text{initial}}$ respectively. Thereafter, the PPFD in the chamber was set to nine \times 3 min flecks of $1500 \mu\text{mol m}^{-2} \text{s}^{-1}$, separated by 1 min low-light periods of $100 \mu\text{mol m}^{-2} \text{s}^{-1}$. The maximum A and g_s during the procedure was referred as $A_{\text{max-fleck}}$, and $g_{s,\text{max}}$ respectively. The steady-state A at low-light phase was referred as $A_{\text{min-fleck}}$. Times to 50% and 90% of the maximum photosynthetic rate ($T_{50\%A}$ and $T_{90\%A}$ respectively) were identified as the period between the start of the first high-light level and the time when the first data point exceeded each of the values in turn. Times to 50 and 90% of the maximum g_s ($T_{50\%g_s}$ and $T_{90\%g_s}$) were calculated similarly.

Integrated carbon gain was calculated as the integrated photosynthesis within 36 min from shifting to a high light level to the end of the ninth low light period. Driven by pools of Calvin cycle intermediates as well as NADPH, ATP, and proton motive force, after shifting from high to low irradiance, photosynthetic CO_2 fixation continues before dropping below A_{initial} , which is referred as post-irradiance fixation (PIF, grey area in Fig. S2). Because of photorespiratory CO_2 release, A will continue decrease to the values below A_{initial} and finally return to steady-state rates. The white area is referred as photosynthetic CO_2 burst (Fig. S2). The PIF and PIB were calculated according to Leakey *et al.* (2002).

Statistical analysis

One-way analysis of variance (ANOVA) and the least-significant difference (l.s.d.) test were used to assess each of the parameters using Statistix 9 software (Analytical Software).

Results

CO_2 response curve

Under well-watered conditions, with increasing CO_2 supply, A first increased and then reached a plateau when C_i was $\sim 600 \mu\text{mol mol}^{-1}$ in both cultivars (Fig. 1). This suggested that CO_2 saturation points were similar between the two

cultivars. Moreover, CO_2 compensation point in Champa was $49.6 \pm 0.3 \mu\text{mol mol}^{-1}$ under well-watered conditions, which was also similar with that in YLY6 ($49.4 \pm 0.9 \mu\text{mol mol}^{-1}$). Under well-watered conditions, CE and A_{steady} were significantly higher in Champa than those in YLY6, whereas $C_{i,\text{steady}}$ was similar between the two cultivars (Table 1). This suggested that mesophyll conductance and/or Rubisco carboxylation capacity was higher in Champa than in YLY6. In fact, V_{cmax} and $g_{m,\text{steady}}$ were slightly higher in Champa than in YLY6, although they were not statistically significant.

Water deficit significantly decreased A_{steady} , $g_{s,\text{steady}}$, $C_{i,\text{steady}}$, $g_{m,\text{steady}}$ and $C_{c,\text{steady}}$ in both cultivars, and the cultivar YLY6 was shown to be more tolerant to water deficit than Champa (Table 1). There was a large difference in CO_2 response curves between well-watered and water deficit conditions in Champa (Fig. 1), this suggested that the depression of A_{steady} in Champa under water deficit conditions was related to both stomatal closure and the impairment of mesophyll conductance and biochemical function (Table 1); the difference in CO_2 response curves between well-watered and water deficit conditions was relative smaller in YLY6 (Fig. 1), this suggested that the depression of A_{steady} in YLY6 was mostly related to stomatal closure with slight impairments of mesophyll conductance and biochemical function (Table 1). In fact, Champa showed significant decreases in both $g_{m,\text{steady}}$, V_{cmax} and J_{max} under 20% PEG treatment, while water deficit generally had no or less effects on them in YLY6. Compared with WW treatment, $g_{m,\text{steady}}$ was decreased by 42% under 20% PEG treatment in Champa; there was no significant difference between WW and 20% PEG treatments in YLY6, although it was decreased by 28% under 15% PEG treatment. Compared with WW treatment, V_{cmax} was decreased by 42% under 20% PEG treatment in Champa, while a less decrease of 18% was observed in YLY6.

Induction states of photosynthesis and stomatal conductance

The IS% of both A and g_s declined with an increased period of low-light level in all treatments and cultivars (Fig. 2). Water

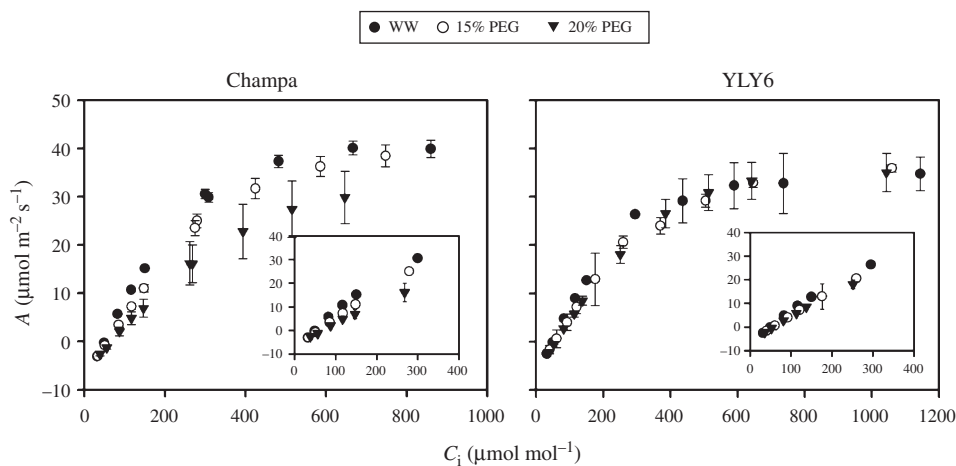


Fig. 1. Effects of PEG-induced water deficit on the CO_2 response curves. Abbreviations: A , leaf photosynthetic rate; C_i , intercellular CO_2 concentration; WW, well-watered condition; 15%PEG, 15% PEG induced water deficit; 20%PEG, 20% PEG induced water deficit.

Table 1. Effects of PEG-induced water deficit on steady-state photosynthetic rate (A_{steady}), stomatal conductance ($g_{\text{s,steady}}$), intercellular CO_2 concentration ($C_{\text{i,steady}}$), mesophyll conductance ($g_{\text{m,steady}}$), chloroplast CO_2 concentration ($C_{\text{c,steady}}$), carboxylation efficiency (CE), maximum Rubisco carboxylation capacity (V_{cmax}) and maximum electron transport capacity (J_{max})

Steady-state gas exchange was measured at a photosynthetic photon flux density (PPFD) of $1500 \mu\text{mol m}^{-2} \text{s}^{-1}$, a CO_2 concentration in the reference chamber of $400 \mu\text{mol mol}^{-1}$, a leaf temperature of 28°C , and a leaf-to-air vapour pressure deficit (VPD) of 1kPa . CO_2 concentration in the reference chamber was controlled across a series of 400, 200, 150, 100, 50, 25, 400, 600, 800, 1000 and $1500 \mu\text{mol mol}^{-1}$ with a CO_2 mixture. Significant differences at the $P < 0.05$ level in each column are followed by different letters. Abbreviations: WW, well-watered condition; 15% PEG, 15% PEG induced water deficit; 20% PEG, 20% PEG induced water deficit

Varieties	Treatments	A_{steady} ($\mu\text{mol m}^{-2} \text{s}^{-1}$)	$g_{\text{s,steady}}$ ($\text{mol m}^{-2} \text{s}^{-1}$)	$C_{\text{i,steady}}$ ($\mu\text{mol mol}^{-1}$)	$g_{\text{m,steady}}$ ($\text{mol m}^{-2} \text{s}^{-1}$)	$C_{\text{c,steady}}$ ($\mu\text{mol mol}^{-1}$)	CE	V_{cmax} ($\mu\text{mol m}^{-2} \text{s}^{-1}$)	J_{max} ($\mu\text{mol m}^{-2} \text{s}^{-1}$)
Champa	WW	$33.7 \pm 0.3\text{a}$	$1.03 \pm 0.05\text{a}$	$310 \pm 3\text{a}$	$0.31 \pm 0.02\text{a}$	$202 \pm 5\text{a}$	$0.156 \pm 0.011\text{a}$	$75.4 \pm 5.0\text{a}$	$229 \pm 9\text{a}$
	15%PEG	$26.0 \pm 1.5\text{bc}$	$0.43 \pm 0.03\text{c}$	$276 \pm 7\text{c}$	$0.25 \pm 0.03\text{bc}$	$171 \pm 14\text{b}$	$0.122 \pm 0.006\text{bc}$	$66.2 \pm 4.0\text{b}$	$224 \pm 9\text{a}$
	20%PEG	$14.9 \pm 0.5\text{d}$	$0.20 \pm 0.02\text{d}$	$257 \pm 18\text{c}$	$0.18 \pm 0.05\text{d}$	$167 \pm 26\text{b}$	$0.090 \pm 0.017\text{e}$	$52.0 \pm 6.5\text{c}$	$194 \pm 22\text{b}$
YLY6	WW	$27.8 \pm 0.5\text{b}$	$0.81 \pm 0.09\text{b}$	$300 \pm 4\text{ab}$	$0.29 \pm 0.03\text{ab}$	$203 \pm 11\text{a}$	$0.130 \pm 0.009\text{b}$	$70.6 \pm 4.8\text{ab}$	$202 \pm 13\text{b}$
	15%PEG	$24.3 \pm 1.0\text{c}$	$0.48 \pm 0.03\text{c}$	$279 \pm 1\text{bc}$	$0.21 \pm 0.02\text{cd}$	$164 \pm 11\text{b}$	$0.109 \pm 0.003\text{cd}$	$57.9 \pm 2.6\text{c}$	$194 \pm 5\text{b}$
	20%PEG	$17.7 \pm 4.7\text{d}$	$0.24 \pm 0.04\text{d}$	$235 \pm 13\text{d}$	$0.28 \pm 0.06\text{ab}$	$170 \pm 13\text{b}$	$0.106 \pm 0.016\text{de}$	$57.8 \pm 6.2\text{c}$	$196 \pm 18\text{b}$

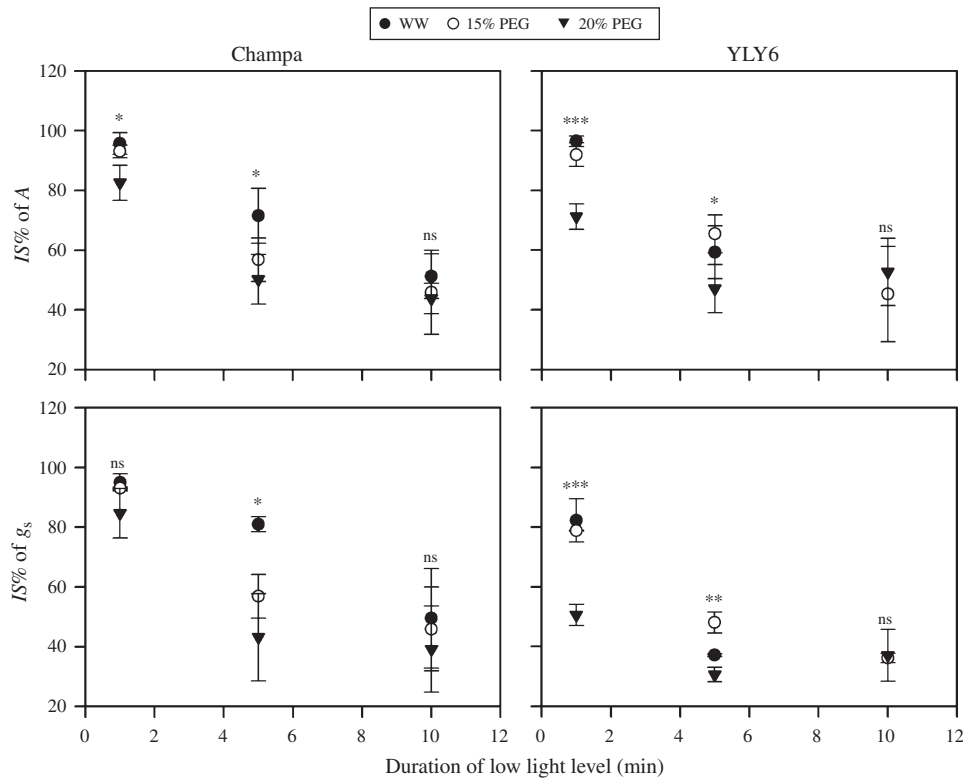


Fig. 2. Effects of PEG-induced water deficit on the responses of $IS\%$ of both A and g_s to various low-light ($100 \mu\text{mol m}^{-2} \text{s}^{-1}$) exposures. Abbreviations: $IS\%$, induction state; A , leaf photosynthetic rate; g_s , stomatal conductance; WW, well-watered condition; 15%PEG, 15% PEG induced water deficit; 20%PEG, 20% PEG induced water deficit. Significant differences are indicated: *, $P < 0.05$; **, $P < 0.01$; ***, $P < 0.001$; ns, not significant at $P < 0.05$ level.

deficit generally decreased the $IS\%$ of both A and g_s after 1 and 5 min of low-light levels, while it had no significant effect after 10 min of low-light. The two cultivars showed similar $IS\%$ of A during the three low-light periods, although Champa possessed a relatively higher $IS\%$ of g_s than YLY6. The $IS\%$ of A was positively related to $IS\%$ of g_s in both cultivars (Fig. 3). The $IS\%$

value of A was higher than the $IS\%$ value of g_s in YLY6, while they were similar in Champa.

There were different patterns in the correlation between the $IS\%$ of A and $g_{\text{s,steady}}$ at different low-light periods (Fig. 4). After 1 min of the low-light level, the $IS\%$ of A was curvilinearly and positively related to $g_{\text{s,steady}}$. The $IS\%$ value of A generally

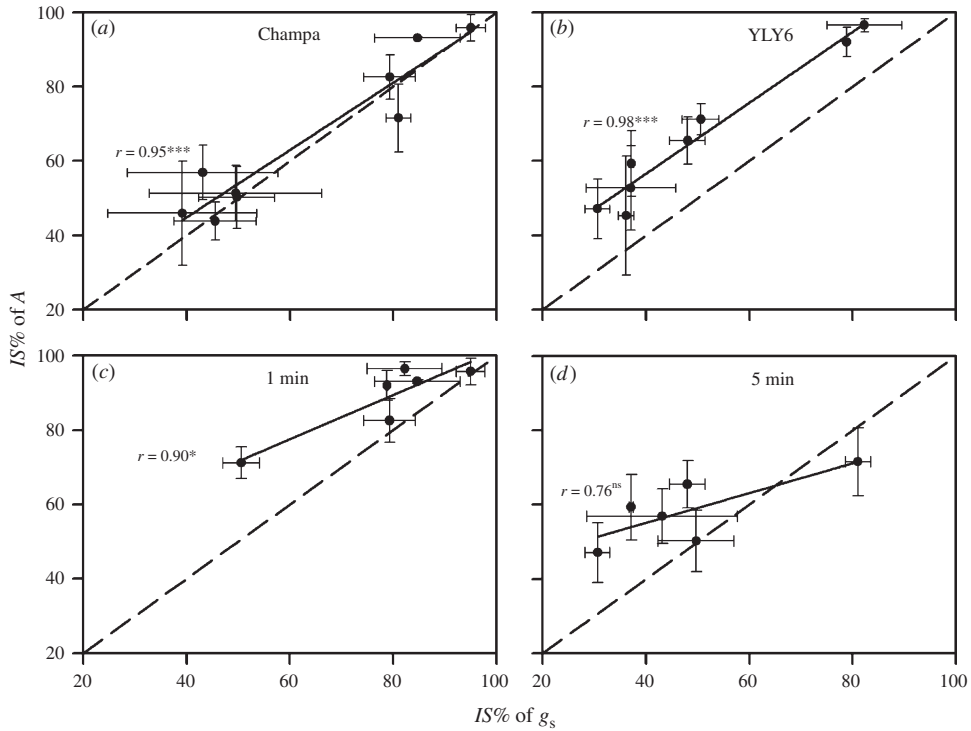


Fig. 3. The correlations between the $IS\%$ of A and the $IS\%$ of g_s in the two cultivars across three different low-light periods (*a, b*), and after different low-light periods within two rice cultivars (*c, d*). Abbreviations: $IS\%$, induction state; A , leaf photosynthetic rate; g_s , stomatal conductance. Significant differences are indicated: ***, $P < 0.001$.

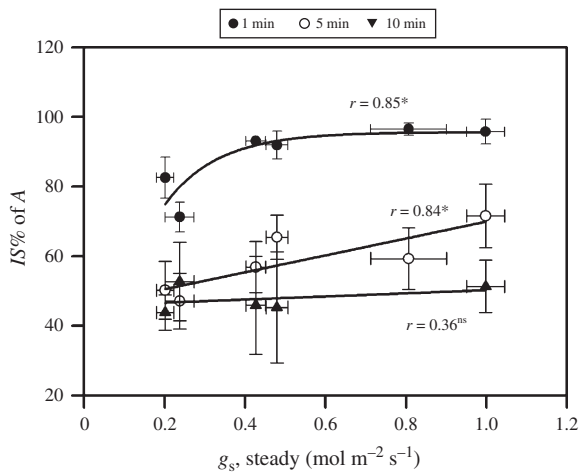


Fig. 4. The correlation between $IS\%$ of A and $g_{s,steady}$ after various duration of the low-light exposures. Abbreviations: $IS\%$, induction state; A , leaf photosynthetic rate; $g_{s,steady}$, steady-state stomatal conductance. Significant differences are indicated: *, $P < 0.05$; ns, not significant at $P < 0.05$.

reached a plateau of 95% when $g_{s,steady}$ was more than $0.4 \text{ mol m}^{-2} \text{ s}^{-1}$, and the $IS\%$ value sharply decreased when $g_{s,steady}$ was less than this threshold. After 5 min of low-light, the $IS\%$ value of A was linearly and positively correlated with $g_{s,steady}$. After 10 min of low-light, no correlation was observed between the $IS\%$ value of A and $g_{s,steady}$, and the $IS\%$ value of A was on average 48% in all treatments.

Dynamic photosynthesis in the flecked irradiance

Compared with well-watered conditions, $A_{max-fleck}$, $A_{min-fleck}$ and $g_{s,max}$ significantly decreased under both water deficit conditions; $A_{initial}$ and $g_{s,initial}$ showed a smaller decrease (Table 2). Water deficit generally had no significant effects on $T_{50\%A}$ and $T_{90\%A}$ on both cultivars, but they were higher in Champer than YLY6, which suggested that Champer requires more time for photosynthesis to recovery after shifting to high light. Water deficit had no significant effect on $T_{50\%g_s}$ in YLY6, but it was significantly decreased under 20% PEG treatment in Champa; water deficit significantly increased $T_{90\%g_s}$ in YLY6, while significantly decreased it in Champa. Water deficit had no significant effect on PIF and PIB, which accounted for 7.84 and 0.17%, respectively, of the integrated CO_2 fixation.

Discussion

For leaves acclimated to shade, photosynthetic response to sudden high irradiance via sunflecks will not be instantaneous, due to downregulation of electron transport processes, deactivation of Calvin cycle enzymes and stomatal closure under shade, and also due to the small size of the pools of Calvin cycle intermediates (Sassenrathcole *et al.* 1994; Tausz *et al.* 2005; Lawson *et al.* 2012). The efficient use of sunflecks is thus dependent on the maintenance of high activation of the enzymes and high stomatal conductance during low-light periods, and also dependent on the rates of both reactivation of enzymes and reopening of stomata. The maintenance of photosynthesis capacity is usually represented using the parameter of the $IS\%$ of

Table 2. Effects of PEG-induced water deficit on steady-state photosynthesis under a low-light level (A_{initial}), maximum photosynthetic rate under flecks ($A_{\text{max-fleck}}$), minimum photosynthetic rate under flecks ($A_{\text{min-fleck}}$), steady-state stomatal conductance under a low-light level ($g_{s,\text{initial}}$), maximum stomatal conductance under flecks ($g_{s,\text{max-fleck}}$), times to 50 and 90% of $A_{\text{max-fleck}}$ ($T_{50\%A}$ and $T_{90\%A}$), times to 50 and 90% of $g_{s,\text{max-fleck}}$ ($T_{50\%g_s}$ and $T_{90\%g_s}$), post-irradiance CO₂ fixation (PIF), and CO₂ burst (PIB)

Data followed by different letters were significant at the $P < 0.05$ level. Abbreviations: WW, well-watered condition; 15% PEG, 15% PEG induced water deficit; 20%PEG, 20% PEG induced water deficit

Parameters	Champa			YLY6		
	WW	15%PEG	20%PEG	WW	15%PEG	20%PEG
A_{initial} ($\mu\text{mol m}^{-2} \text{s}^{-1}$)	6.4 ± 1.0a	6.1 ± 0.4ab	5.3 ± 0.4b	3.5 ± 1.0c	2.0 ± 1.1d	4.0 ± 1.1c
$A_{\text{max-fleck}}$ ($\mu\text{mol m}^{-2} \text{s}^{-1}$)	33.3 ± 1.6a	26.9 ± 1.5bc	18.8 ± 1.5d	28.0 ± 2.4b	24.7 ± 2.5c	19.2 ± 2.5d
$A_{\text{min-fleck}}$ ($\mu\text{mol m}^{-2} \text{s}^{-1}$)	4.18 ± 0.80a	1.42 ± 0.50d	0.16 ± 0.50e	2.94 ± 0.63b	2.53 ± 0.37bc	1.66 ± 0.37cd
$g_{s,\text{initial}}$ ($\text{mol m}^{-2} \text{s}^{-1}$)	0.31 ± 0.02a	0.22 ± 0.06ab	0.18 ± 0.06b	0.12 ± 0.03c	0.05 ± 0.03d	0.13 ± 0.03c
$g_{s,\text{max}}$ ($\text{mol m}^{-2} \text{s}^{-1}$)	1.16 ± 0.23a	0.56 ± 0.09b	0.30 ± 0.09c	0.62 ± 0.10b	0.42 ± 0.14c	0.33 ± 0.14c
$T_{50\%A}$ (min)	1.19 ± 0.18abc	1.49 ± 0.82a	0.87 ± 0.82abc	0.72 ± 0.15bc	1.31 ± 0.67ab	0.49 ± 0.67c
$T_{90\%A}$ (min)	8.7 ± 2.1abc	11.8 ± 2.2a	9.6 ± 2.2ab	2.7 ± 1.1d	3.7 ± 1.2cd	6.5 ± 1.2bcd
$T_{50\%g_s}$ (min)	5.04 ± 0.55a	4.30 ± 3.28a	0.06 ± 0.12b	0.78 ± 0.20b	1.27 ± 0.71b	0.40 ± 0.04b
$T_{90\%g_s}$ (min)	16.0 ± 8.4a	17.8 ± 3.3a	4.3 ± 2.6bc	1.9 ± 0.9c	2.7 ± 1.5bc	7.3 ± 1.7b
PIF (%)	7.8 ± 0.2a	8.2 ± 0.8a	7.6 ± 0.8a	6.1 ± 0.3b	5.5 ± 0.5b	6.5 ± 0.5b
PIB (%)	0.13 ± 0.11a	0.06 ± 0.09a	0.32 ± 0.09a	0.30 ± 0.10a	0.47 ± 0.06a	0.50 ± 0.06a

A , due to the positive correlation between $IS\%$ of A and integrated CO₂ assimilation (Naumburg and Ellsworth 2000). The $IS\%$ of A is reported to be negatively related to duration of shade or low-light periods, and to be environment- and species-dependent (Leakey et al. 2002; Kubásek et al. 2013). High temperature stress can significantly decrease the $IS\%$ of A (Leakey et al. 2003), while CO₂ enrichment can increase it (Leakey et al. 2002). The present study demonstrated that water deficit can decrease $IS\%$ of both A and g_s , which were generally decreased with increasing periods of low light between 1 and 10 min (Fig. 2).

The $IS\%$ of A and $IS\%$ of g_s are highly correlated and of a similar magnitude (Leakey et al. 2002). In the present study, the $IS\%$ of A and $IS\%$ of g_s were highly correlated across three different low-light periods in both cultivars, with the same magnitude in Champa and a lower magnitude of the $IS\%$ of g_s in YLY6 (Fig. 3a, b). However, these high correlations is largely due to the decline of $IS\%$ with the duration of low-light period. To remove the time factor, the correlations between $IS\%$ of A and $IS\%$ of g_s after different low-light periods were created (Fig. 3c, d). It showed that $IS\%$ of A is positively related to $IS\%$ of g_s after 1 and 5 min of low-light periods, although the correlation is not significant at $P < 0.05$ level after 5 min low-light period ($r = 0.76$, $P = 0.077$). The $IS\%$ of A was not related to $IS\%$ of g_s after 10 min of low-light period (Data not shown). This suggested that, the maintenance of photosynthesis under a short period of low-light (<5 min) is highly correlated with the maintenance of stomatal conductance, but may related to the biochemical function of Calvin cycle enzymes under a long period of low-light (>5 min).

The $IS\%$ of A is reported to be positively related to $g_{s,\text{steady}}$ (Allen and Pearcy 2000). In the present study, $IS\%$ of A was positively related to $g_{s,\text{steady}}$ after 1 and 5 min of low-light level (Fig. 4). However, $IS\%$ of A was not related to $g_{s,\text{steady}}$ after 10 min of low-light level, probably because of the similar $IS\%$ of g_s between well-watered and water deficit conditions.

Numerous studies have shown that the time required for photosynthesis induction is less than that required for stomatal induction (Leakey et al. 2002, 2003; Lawson et al. 2012). This suggests that the recovery rate of Calvin cycle enzymes is faster

than stomatal conductance, although the activation of these two processes seemed to be highly coordinated, and photosynthesis is limited more by stomatal conductance during the photosynthesis induction process. With the cultivar of Champer, the times required for photosynthesis induction ($T_{50\%A}$ and $T_{90\%A}$) were less than stomatal induction ($T_{50\%g_s}$ and $T_{90\%g_s}$) under well-watered and 15% PEG treatments, but were longer than those for stomatal induction under 20% PEG treatment (Table 2). This suggested that, during the induction process, the induction of biochemical capacity was faster than stomatal conductance under well-watered and 15% PEG treatments; in reverse, the induction of biochemical capacity was slower than stomatal conductance under 20% PEG treatment as the biochemical capacity (e.g. V_{cmax} and J_{max}) is impaired (Table 1). With the cultivar of YLY6, the times required for photosynthesis induction were comparable with stomatal induction, which suggested that, during the induction process, the photosynthesis is mainly limited by stomatal conductance.

After shifting from high to low irradiance, photosynthesis will not directly fall to a new steady-state, but its decrease lags behind for a few seconds (Fig. S2). This phenomenon, termed PIF in the present study, is driven by pools of Calvin cycle intermediates as well as NADPH, ATP, and proton motive force (Sharkey et al. 1986; Kaiser et al. 2015). PIB is caused by a transient rise in photorespiratory CO₂ production, and is related to a lag time between adjustment of photorespiratory 2-phosphoglycolate recycling relative to Calvin cycle cycling (Prinsley et al. 1986; Kaiser et al. 2015). Leakey et al. (2002) showed that PIF and PIB account for 18.1 and 0.56%, respectively, of the integrated CO₂ fixation in *Shorea leprosula* at atmospheric CO₂ concentration, and elevated CO₂ concentration can lead to 14% increase and 88% decrease, respectively, of them. In the present study, the averages of 7.0 and 0.30% of PIF and PIB were observed in rice plants, and water deficit had no significant effect on them.

Leakey et al. (2003) reported that the $A_{\text{min-fleck}}$ is lower than the A_{initial} , which will decrease the integrated CO₂ fixation and light use efficiency under flecked irradiance. This phenomenon was also observed in the present study, especially under drought stress

(Table 2), which suggested that flecked irradiance will aggravate the negative effect of water deficit on photosynthesis. Kromdijk *et al.* (2016) illustrated that the difference between $A_{\text{min-fleck}}$ and A_{initial} is caused by the protective dissipation of non-photochemical quenching (NPQ). Moreover, the mobility of chloroplasts is likely another reason. Chloroplasts mostly accumulate in low-light surfaces to absorb more light, and move away from strong light surfaces to avoid damage caused by the absorption of excess light (Banaš *et al.* 2012; Wada 2013). After exposure to high-light periods, the leaves would then allocate more chloroplasts vertically towards the leaf surface in low-light periods under flecked irradiance than under conditions of same light intensity of continuously low-light irradiance periods. This would potentially result in a lower light absorption and photosynthesis.

In conclusion, water deficit significantly decreases the maintenance of photosynthetic capacity and stomatal conductance under low-light periods, and the $IS\%$ of both A and g_s were generally decreased with increasing periods of low light between 1 and 10 min. Water deficit generally had no significant effect on the time required for photosynthesis induction after exposure to high-light levels, but led to a significantly greater decrease in $A_{\text{min-fleck}}$ relative to A_{initial} . The lower $IS\%$ of A and more severe decrease in $A_{\text{min-fleck}}$ relative to A_{initial} suggest that the inhibition of photosynthesis under water deficit is greater under flecked irradiance.

Acknowledgements

This work was supported by the National Key Research and Development Program of China (2016YFD0300102), National Natural Science Foundation of China (31301840), A Foundation for the Author of National Excellent Doctoral Dissertation of PR China (201465), and Fundamental Research Funds for the Central Universities (2662015PY031).

References

- Allen MT, Pearcy RW (2000) Stomatal versus biochemical limitations to dynamic photosynthetic performance in four tropical rainforest shrub species. *Oecologia* **122**, 479–486. doi:10.1007/s004420050969
- Banaš AK, Aggarwal C, Iabuz J, Sztatelman O, Gabryś H (2012) Blue light signalling in chloroplast movements. *Journal of Experimental Botany* **63**, 1559–1574. doi:10.1093/jxb/err429
- Bernacchi CJ, Portis AR, Nakano H, von Caemmerer S, Long SP (2002) Temperature response of mesophyll conductance. Implications for the determination of Rubisco enzyme kinetics and for limitations to photosynthesis *in vivo*. *Plant Physiology* **130**, 1992–1998. doi:10.1104/pp.008250
- Cano FJ, López R, Warren CR (2014) Implications of the mesophyll conductance to CO₂ for photosynthesis and water-use efficiency during long-term water stress and recovery in two contrasting Eucalyptus species. *Plant, Cell & Environment* **37**, 2470–2490. doi:10.1111/pce.12325
- Cui X, Gu S, Wu J, Tang Y (2009) Photosynthetic response to dynamic changes of light and air humidity in two moss species from the Tibetan Plateau. *Ecological Research* **24**, 645–653. doi:10.1007/s11284-008-0535-8
- Farquhar GD, von Caemmerer S, Berry JA (1980) A biochemical model of photosynthetic CO₂ assimilation in leaves of C₃ species. *Planta* **149**, 78–90. doi:10.1007/BF00386231
- Flexas J, Medrano H (2002) Drought-inhibition of photosynthesis in C₃ plants: stomatal and non-stomatal limitations revisited. *Annals of Botany* **89**, 183–189. doi:10.1093/aob/mcf027
- Flexas J, Bota J, Escalona JM, Sampol B, Medrano H (2002) Effects of drought on photosynthesis in grapevines under field conditions: an evaluation of stomatal and mesophyll limitations. *Functional Plant Biology* **29**, 461–471. doi:10.1071/PP01119
- Hubbart S, Peng SB, Horton P, Chen Y, Murchie EH (2007) Trends in leaf photosynthesis in historical rice varieties developed in the Philippines since 1966. *Journal of Experimental Botany* **58**, 3429–3438. doi:10.1093/jxb/erm192
- Kaiser E, Morales A, Harbinson J, Kromdijk J, Heuvelink E, Marcelis LF (2015) Dynamic photosynthesis in different environmental conditions. *Journal of Experimental Botany* **66**, 2415–2426. doi:10.1093/jxb/eru406
- Kromdijk J, Glowacka K, Leonelli L, Gabilly ST, Iwai M, Niyogi KK, Long SP (2016) Improving photosynthesis and crop productivity by accelerating recovery from photoprotection. *Science* **354**, 857–861. doi:10.1126/science.aai8878
- Kubásek J, Urban O, Šantrůček J (2013) C₄ plants use fluctuating light less efficiently than do C₃ plants: a study of growth, photosynthesis and carbon isotope discrimination. *Physiologia Plantarum* **149**, 528–539. doi:10.1111/ppl.12057
- Lawson T, Kramer DM, Raines CA (2012) Improving yield by exploiting mechanisms underlying natural variation of photosynthesis. *Current Opinion in Biotechnology* **23**, 215–220. doi:10.1016/j.copbio.2011.12.012
- Leakey ADB, Press MC, Scholes JD, Watling JR (2002) Relative enhancement of photosynthesis and growth at elevated CO₂ is greater under sunflecks than uniform irradiance in a tropical rain forest tree seedling. *Plant, Cell & Environment* **25**, 1701–1714. doi:10.1046/j.1365-3040.2002.00944.x
- Leakey ADB, Press MC, Scholes JD (2003) Patterns of dynamic irradiance affect the photosynthetic capacity and growth of dipterocarp tree seedlings. *Oecologia* **135**, 184–193. doi:10.1007/s00442-003-1178-7
- Li Y, Ren BB, Yang XX, Xu GH, Shen QR, Guo SW (2012) Chloroplast downsizing under nitrate nutrition restrained mesophyll conductance and photosynthesis in rice (*Oryza sativa* L.) under drought conditions. *Plant & Cell Physiology* **53**, 892–900. doi:10.1093/pcp/pcs032
- Naumburg E, Ellsworth DS (2000) Photosynthetic sunfleck utilization potential of understory saplings growing under elevated CO₂ in FACE. *Oecologia* **122**, 163–174. doi:10.1007/PL00008844
- Parry MAJ, Andralojc PJ, Khan S, Lea PJ, Keys AJ (2002) Rubisco activity: effects of drought stress. *Annals of Botany* **89**, 833–839. doi:10.1093/aob/mcf103
- Pearcy RW, Roden JS, Gamon JA (1990) Sunfleck dynamics in relation to canopy structure in a soybean (*Glycine max* (L.) Merr.) canopy. *Agricultural and Forest Meteorology* **52**, 359–372. doi:10.1016/0168-1923(90)90092-K
- Perez-Martin A, Michelazzo C, Torres-Ruiz JM, Flexas J, Fernández JE, Sebastiani L, Diaz-Espejo A (2014) Regulation of photosynthesis and stomatal and mesophyll conductance under water stress and recovery in olive trees: correlation with gene expression of carbonic anhydrase and aquaporins. *Journal of Experimental Botany* **65**, 3143–3156. doi:10.1093/jxb/eru160
- Prinsley RT, Hunt S, Smith AM, Leegood RC (1986) The influence of a decrease in irradiance on photosynthetic carbon assimilation in leaves of *Spinacia oleracea* L. *Planta* **167**, 414–420. doi:10.1007/BF00391348
- Sassenrath-Cole GF, Pearcy RW, Steinmaus S (1994) The role of enzyme activation state in limiting carbon assimilation under variable light conditions. *Photosynthesis Research* **41**, 295–302. doi:10.1007/BF00019407
- Sharkey TD (2016) What gas exchange data can tell us about photosynthesis. *Plant, Cell & Environment* **39**, 1161–1163. doi:10.1111/pce.12641
- Sharkey TD, Seemann JR, Pearcy RW (1986) Contribution of metabolites of photosynthesis to postillumination CO₂ assimilation in response to lightflecks. *Plant Physiology* **82**, 1063–1068. doi:10.1104/pp.82.4.1063
- Sharkey TD, Bernacchi CJ, Farquhar GD, Singsaas EL (2007) Fitting photosynthetic carbon dioxide response curves for C₃ leaves. *Plant,*

- Cell & Environment* **30**, 1035–1040. doi:[10.1111/j.1365-3040.2007.01710.x](https://doi.org/10.1111/j.1365-3040.2007.01710.x)
- Sun JL, Ye M, Peng SB, Li Y (2016) Nitrogen can improve the rapid response of photosynthesis to changing irradiance in rice (*Oryza sativa* L.) plants. *Scientific Reports* **6**, 31305. doi:[10.1038/srep31305](https://doi.org/10.1038/srep31305)
- Tausz M, Warren CR, Adams MA (2005) Dynamic light use and protection from excess light in upper canopy and coppice leaves of *Nothofagus cunninghamii* in an old growth, cool temperate rainforest in Victoria, Australia. *New Phytologist* **165**, 143–156. doi:[10.1111/j.1469-8137.2004.01232.x](https://doi.org/10.1111/j.1469-8137.2004.01232.x)
- Timm HC, Stegemann J, Küppers M (2002) Photosynthetic induction strongly affects the light compensation point of net photosynthesis and coincidentally the apparent quantum yield. *Trees* **16**, 47–62. doi:[10.1007/s004680100123](https://doi.org/10.1007/s004680100123)
- Valentini R, Epron D, Deangelis P, Matteucci G, Dreyer E (1995) *In situ* estimation of net CO₂ assimilation, photosynthetic electron flow and photorespiration in turkey oak (*Q. cerris* L.) leaves. Diurnal cycles under different levels of water-supply. *Plant, Cell & Environment* **18**, 631–640. doi:[10.1111/j.1365-3040.1995.tb00564.x](https://doi.org/10.1111/j.1365-3040.1995.tb00564.x)
- Valladares F, Allen MT, Pearcy RW (1997) Photosynthetic responses to dynamic light under field conditions in six tropical rainforest shrubs occurring along a light gradient. *Oecologia* **111**, 505–514. doi:[10.1007/s004420050264](https://doi.org/10.1007/s004420050264)
- Wada M (2013) Chloroplast movement. *Plant Science* **210**, 177–182. doi:[10.1016/j.plantsci.2013.05.016](https://doi.org/10.1016/j.plantsci.2013.05.016)
- Way DA, Pearcy RW (2012) Sunflecks in trees and forests: from photosynthetic physiology to global change biology. *Tree Physiology* **32**, 1066–1081. doi:[10.1093/treephys/tps064](https://doi.org/10.1093/treephys/tps064)
- Wong SL, Chen CW, Huang HW, Weng JH (2012) Using combined measurements for comparison of light induction of stomatal conductance, electron transport rate and CO₂ fixation in woody and fern species adapted to different light regimes. *Tree Physiology* **32**, 535–544. doi:[10.1093/treephys/tps037](https://doi.org/10.1093/treephys/tps037)